

EFFECT OF FREQUENCY FROM "LOW FREQUENCY" TO MICROWAVE ON THE  
PLASMA DEPOSITION OF THIN FILMS

M.R. Wertheimer<sup>1</sup>, M. Moisan<sup>2</sup>, J.E. Klemberg-Sapieha<sup>1</sup> and R. Claude<sup>1,2</sup>  
<sup>1</sup>"Groupe des Couches Minces" and Department of Engineering Physics, Ecole Poly-  
technique, Box 6079, Station "A", Montréal Québec H3C 3A7, Canada  
<sup>2</sup>Département de Physique, Université de Montréal, Montréal, Québec H3C 3J7

ABSTRACT

Theory predicts that the electron energy distribution function (EEDF) of a high frequency, low pressure plasma is modified when the parameter  $\nu/\omega$  is greater (radio frequency, "RF" case) or less (microwave, "MW" case) than unity ( $\nu$  is the effective average electron-neutral collision frequency for momentum transfer). In argon at 200 mTorr, the calculated value of  $\nu/2\pi$  is about 50 MHz. Assuming that this applies also to molecular gases, we have used two different plasma systems for thin film deposition experiments in which frequency of the applied field  $f (= \omega/2\pi)$  was the only variable. In all cases studied, deposition rate  $R$  was substantially lower in the "RF" than in the "MW" regime: ( $R_{MW}/R_{RF}$ ) values were about 5, 10 and 20 for deposition of plasma polymers, P-SiN and a-Si:H, respectively, in agreement with the few published data in the literature. Microwave plasmas therefore appear more attractive for industrial processing where throughput is a principal consideration.

1. INTRODUCTION

It is now well accepted that parameters such as gas pressure, flow rate and composition, reactor design and power density deposited in the plasma, can strongly influence a given plasma etch or deposition process. However, the situation is quite different regarding the action of the applied field frequency  $f (= \omega/2\pi)$  for high frequency (HF) sustained plasmas: some authors feel that there is no frequency effect or that it is negligible, some prefer to ignore the question to obviate the need to redesign or optimize their reactor, while among those who accept that  $f$  plays a rôle in plasma processing, there are contradictory statements as to its exact influence. This situation can readily be explained by insufficient experimental information and insufficient plasma modeling. Manufacturers' conservatism, until very recently, is illustrated by the fact, as noted by Flamm(1), that equipment was designed to operate at one or the other of a few FCC licensed industrial frequencies (e.g. 13.56 MHz), and that consequently  $f$  has only rarely been figured into the design of apparatus for process applications. To our knowledge, there is presently no commercial reactor with provisions for process optimization by varying  $f$ . In fact, the intentional exploitation of this variable as a process parameter for etching or deposition is a recent line of research, as indicated by the contents of two review papers on the subject(1,2).

remaining parts, is at ground potential). Consequently, among all the external plasma variables mentioned in the Introduction, in this experiment,  $f$  as well as the sheath potential, are varied in changing from configuration 2(a) to 2(b). Comparing the RF electroded configuration with an electrodeless MW discharge is important, as it corresponds to the two most commonly used types of discharges. However, one must bear in mind that the influence of sheath-induced ion bombardment in the case of the electroded reactor introduces an additional parameter into frequency comparison. Evidently, 2(b) could be operated over a relatively broad RF frequency range with the appropriate power supply and matching network, but this has not yet been done.

### 2.3 Characterization of Thin Film Deposits

So far the principal use of apparatus described in section 2.1 has been to study the deposition kinetics of hydrocarbon and fluorocarbon plasma polymers(17,18), although systematic investigations of resulting film characteristics have commenced.

Apparatus described in section 2.2, on the other hand, is used continually for depositing various thin film materials, which are then carefully characterized by a variety of physical and chemical techniques, depending on their end use. Families of thin film materials which have been thus prepared and studied are

- (i) Plasma polymers, particularly organo-silicones(15,19,20);
- (ii) Inorganic silicon compounds (silicon nitride, oxide and oxynitride)(21) and
- (iii) amorphous hydrogenated silicon.

## 3. RESULTS AND DISCUSSION

The results presented here are primarily concerned with illustrating the effect of  $f$  upon deposition kinetics of various thin film materials mentioned above. Where appropriate, characterization data are also presented.

### 3.1 Organic Materials (Plasma Polymers)

Probably the most conclusive demonstration so far of frequency-dependent effects in low pressure HF plasma processing is the work of Claude et al.(17,18) on plasma polymerization of hydrocarbon and fluorocarbon monomers. Figure 3 shows a plot of  $\log(R/P)$  vs.  $f$  for isobutylene (IB, upper curve) and perfluorocyclobutane (PFCB, lower curve), where  $R$  is deposition rate (in  $\text{\AA min}^{-1}$ ) and  $P$  is the power absorbed by the plasma. It must be emphasized that under the conditions of the experiment, plasma volume was constant, so that  $P$  is proportional to power density in the plasma: the full circles and cross symbols on the upper plot, which pertain to different power values at any given frequency, clearly indicate that the observed effects are due only to variation of  $f$  (pressure, flow rate, and other pertinent parameters having been kept constant throughout). Figure 3 reveals a number of important features: the IB curve clearly displays two plateaus, one at low frequencies ( $f < 30$  MHz), the other at high frequencies ( $f > 100$  MHz), the  $R/P$  value of the former being about a factor of 5 lower than the latter. In the case of PFCB, there is a plateau for  $f > 100$  MHz, but  $R/P$  still appears to be decreasing at the lowest frequency (12 MHz) investigated here. The most striking and important feature of this plot, however, is the fact that the transition region between the RF and "microwave" plateaus appears to be centred at  $v/\omega \approx 1$ , in agreement with the theoretical model as to the role played by the EEDF(2,7).

There exist various types of physical phenomena that can be responsible for frequency effects in process plasmas. When considering  $f \geq 10$  or 20 MHz, one can ignore lower frequency phenomena such as the ion-sheath transit effects(1), and one can point to two remaining important frequency-dependent phenomena: modifications to the shape of the electron energy distribution function (EEDF)(2), and changes in the spatial distribution of the HF field intensity. The latter effect, which evidently has bearing on the spatial distributions of excited species, for example chemically active precursors, is the object of detailed discussions in recent work by Ricard et al.(3-6). The former phenomenon, particularly investigation of the dependence of the EEDF on  $\nu/\omega$ (2,7) ( $\nu$  is the effective average electron-neutral collision frequency for momentum transfer) is connected with energy selectivity within the multitude of chemical reactions occurring in typical process plasmas. In the present paper, we review experimental observations, mostly from our own laboratories and all relating to thin film deposition studies, which appear connected with changes in the EEDF as  $\nu/\omega$  is varied. Films have been characterized as to their structures and relevant physico-chemical properties; when significant property variations occurred with varying  $f$ , these are specifically emphasized.

## 2. EXPERIMENTAL (APPARATUS FOR VARYING FREQUENCY)

A major problem when performing frequency-dependent investigation is to ensure that truly the only external parameter being varied is the applied frequency. As a rule, reactors designed for radio frequency (RF) plasmas are different from those operated with microwaves. Since reactor walls, particularly important in tubular configurations (i.e. large length to radius ratio), are completely (ambipolar diffusion case) or partially (volume recombination case) responsible for the plasma loss rate, no true frequency effect comparison can be made if the prevailing condition is not rigorously maintained. The results presented below have been obtained using two different techniques for producing HF plasmas, both using the same reactor geometry and volume at R.F. and microwave frequencies, as well as the same power densities, pressures and gas flows; they are (i) the surface wave plasma and (ii) the "large volume microwave" (LMP) plasma techniques.

### 2.1 Surface Wave Plasma Apparatus

Surface wave produced plasma columns are sustained by the electric field of an electromagnetic surface wave that uses the plasma column and the dielectric tube containing it as its sole propagating structure: there is thus no need for an applicator that would run along the discharge tube to activate it. The power flowing along the plasma tube is emitted by a compact, localized, wave launching gap device. Such plasma columns can be sustained with the same electromagnetic field configuration (the azimuthally symmetric mode of propagation) over an extremely broad range of frequency (4 MHz - 10 GHz demonstrated): this ensures that the only external parameter varied is the applied frequency. A further advantage of surface wave plasmas for such studies is that modelling is very well developed: the field intensity distribution, the electron density (axial and radial distributions) as well as the dispersion and attenuation properties of the wave can be calculated(8,9) (For a review on surface wave plasma properties, see Refs. 9,10).

There now exist a large variety of surface wave launchers(11-14) which allow one to operate in the RF as well as in the microwave frequency range, at power levels ranging from a hundred watts to kilowatts with discharge tube diameters ranging from 0.5 mm to 150 mm (demonstrated). The operating conditions can be chosen, or the launcher tuned, so that only the azimuthally symmetric mode of propagation is excited, yielding a plasma column with properties which are independent of the particular launcher used.

microwave energy is supplied to the plasma from the 30 cm long strapped-bar slow wave structure(16). Substrates to be coated are mounted facing downward on the underside of the heated sample holder (15 cm diameter), the distance of which to the silica window plate can be adjusted vertically. Usually this spacing is 4 cm, so that the total plasma volume in the contained space is about 1600 cm<sup>3</sup>.

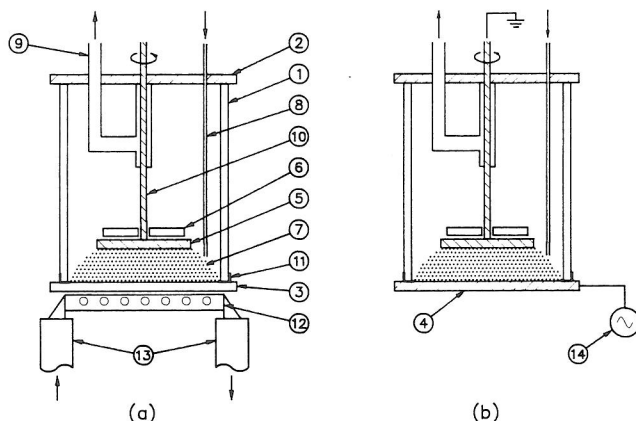


Fig. 2 : Plasma system based on LMP: (a) microwave ("MW") mode system, operating at 2.45 GHz; (b) radiofrequency ("RF") mode system, operating at 13.56 MHz.

- 1 Pyrex reactor wall;
- 2 stainless steel top plate;
- 3 microwave window plate;
- 4 powered electrode;
- 5 rotating substrate holder (at ground potential);
- 6 heating element;
- 7 plasma;
- 8 reagent gas feed line;
- 9 pumping line;
- 10 rotating shaft (to ground);
- 11 vacuum seal;
- 12 slow wave microwave applicator;
- 13 input and output waveguides;
- 14 RF generator and matching network.

Figure 2(b) shows this reactor system in the "RF" mode of operation; this modification is accomplished with ease by removing the microwave applicator and replacing the silica glass window by a polished stainless steel plate of the same dimensions. This metal plate is electrically connected to the 13.56 MHz power supply and matching network, and thereby becomes the "powered" electrode of a capacitively coupled discharge system, the "grounded" electrode being the sample holder (which, along with the metal top plate and all the

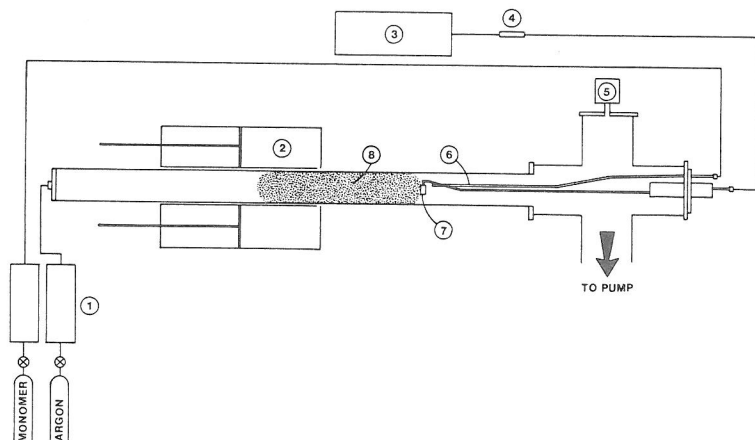


Fig. 1 : Plasma system based on the surface wave technique.

- 1 Mass flow controllers;
- 2 surface wave launcher;
- 3 microbalance readout unit;
- 4 low-pass filter;
- 5 capacitive vacuum gauge;
- 6 monomer injector;
- 7 microbalance quartz crystal detector (substrate);
- 8 plasma.

Figure 1 shows the surface wave discharge setup used for the plasma polymerization experiments. The discharge tube is a cylindrical pyrex tube (61 mm i.d.) and the substrate holder (a quartz crystal mass detector) is oriented perpendicularly to the wave propagation direction. The plasma column length depends on the HF power supplied to the wave launcher; the power can be set so that the plasma barely reaches the substrate while, for larger power levels, the wave will be totally reflected at the substrate, increasing the plasma density on its way back toward the launcher. For still larger power, part of the wave power flows around the substrate, producing plasma beyond the substrate. The experiments reported hereunder were performed under reflection conditions, with the plasma occupying a constant volume, as the plasma column was maintained between the substrate holder location and the launcher.

## 2.2 Plasma Apparatus based on LMP

Figure 2 shows a second reactor system for frequency-dependent studies; unlike that discussed in section 2.1, it has been used only at two industrial frequencies, namely 13.56 ("RF") and 2450 MHz ("MW"). Figure 2(a) shows this "bell jar" type of reactor in the "MW" mode; as it has already been described elsewhere(15), only the most important features are discussed here. The reactor vessel consists of a 23 cm diameter, 19 cm high Pyrex cylinder with a stainless steel top plate incorporating all the required access connections (rotating vacuum seal for the sample holder and electrical feedthroughs for its heater, connection to the turbomolecular pump, Baratron vacuum gauge, gas inlet from the electronic mass flow meters, etc.). The bottom of the reactor consists of a 27.5 cm diameter, 1.3 cm thick fused silica "window" through which

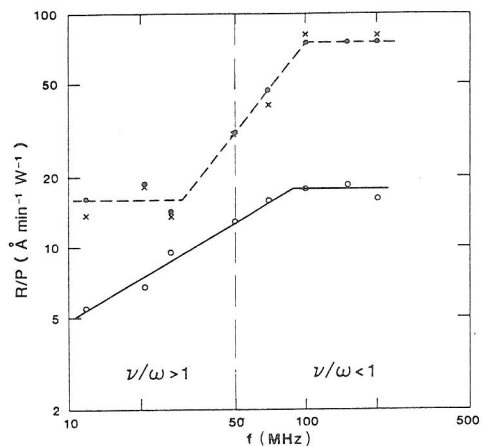


Fig. 3.  
Plot of  $\log(R/P)$  versus  $\log(\text{excitation frequency})$ , where  $R$  is deposition rate and  $P$  is absorbed power. The upper curve pertains to plasma polymerized isobutylene (x "low" power o: "high" power), the lower to plasma polymerized perfluorocyclobutane (o: "high" power).

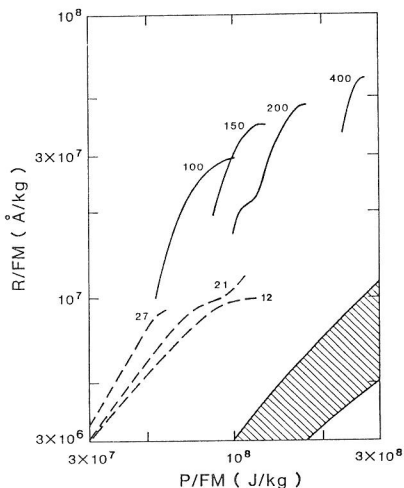


Fig. 4.  
Plot of  $R/FM$  vs. the composite parameter  $P/FM$  (see text), for perfluorocyclobutane, at RF ( $\leq 27$  MHz) and microwave ( $> 100$  MHz) frequencies. The hatched zone is from Gazicki and Yasuda(23) for fluorocarbons, at audio-frequency.

In Figure 4, results for PFCB are presented in a plot of composite parameters  $R/FM$  vs.  $P/FM$ , as first proposed by Yasuda(22),  $F$  and  $M$  being flow rate and molecular weight of the monomer, respectively. The solid and broken curves represent the indicated "microwave" and "low" frequencies, respectively, while the hatched region pertains to the 10 kHz data of Gazicki and Yasuda(23) for various fluorocarbon monomers. If we consider an (imaginary) envelope curve connecting the maxima of the solid curves with its counterpart for the broken curves, the "microwave" data are again about 5 times higher than the "low" frequency data, for a given  $P/FM$  value (e.g.  $10^8$  J/kg). The horizontal shift along the abscissa (by a factor of about 3) between Gazicki's and Claude's "low" frequency data is due to the fact that the experiments were carried out in very different reactor geometries, beside other differences in experimental methodologies. For more details, the reader is referred to the respective references.

### 3.2 Inorganic Materials

In this section, we report frequency-dependent results relating to amorphous hydrogenated silicon films (a-Si:H) prepared from silane/argon ( $\text{SiH}_4/\text{Ar}$ ) gas mixtures, and to "plasma silicon nitride" (P-SiN: actually a-SiN<sub>x</sub>:H) films prepared from silane/ammonia ( $\text{SiH}_4/\text{NH}_3$ ) gas mixtures.

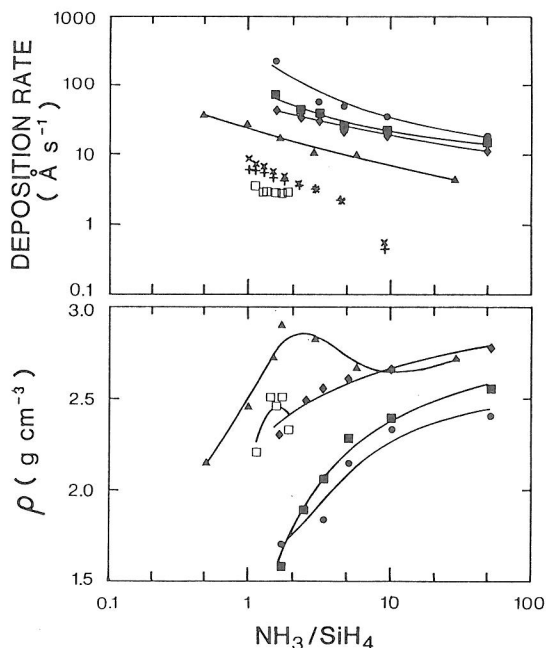


Fig. 5 Composite plot of data derived from the present work, and their comparison with results from the literature. The abscissa is  $\log$  (ratio of  $\text{NH}_3$  to  $\text{SiH}_4$  flowrates), as described in the text. Full symbols relate to the present sample series (see text):  $\bullet$  "A",  $T = 25^\circ\text{C}$ ;  $\blacksquare$  "B",  $T = 100^\circ\text{C}$ ;  $\blacklozenge$  "C",  $T = 200^\circ\text{C}$ ;  $\blacktriangle$  "D",  $T = 250^\circ\text{C}$ . Other symbols:  $\square$  Sinha, (24);  $\times$  and  $+$  Kaganowicz (24), 400W and 100W, respectively.

First, regarding the latter material, Fig. 5 shows a composite plot with a common abscissa,  $\log[(\text{NH}_3/\text{SiH}_4)]$ , the flow rate ratio, of data pertaining to four sample series A to D, and of selected data from the literature. Series A to D were prepared in the reactor of Fig. 2(a), at substrate temperatures  $T_s = 25, 100, 200$  and  $250^\circ\text{C}$ , respectively. No P-SiN preparation has so far been carried out in the 2(b) configuration. For comparison, we also show data of Kaganowicz and Robinson (24) ( $f = 13.56$  MHz,  $T_s < 40^\circ\text{C}$ ) and Sinha et al. (25) ( $f = 13.56$  MHz,  $T_s = 275^\circ\text{C}$ ). In Fig. 5(a), we plot  $\log$  [deposition rate], while 5(b) shows a plot of film densities. In (a) the deposition rate, at a given value of  $T_s$ , is seen to decrease with increasing  $(\text{NH}_3/\text{SiH}_4)$  ratio. This is to be expected, as the increase in this ratio is achieved by reducing  $\text{SiH}_4$  flow rate (21); also expected is the observed drop in  $R$  (at constant  $\text{NH}_3/\text{SiH}_4$ ) with rising  $T_s$ . The data of Kaganowicz (24) and of Sinha et al. (25) show similar trends, but their deposition rates (for  $T_s < 40^\circ\text{C}$  and  $275^\circ\text{C}$ , respectively) are factors of  $\sim 25$  and  $\sim 10$  lower than the present results, under comparable fabrication conditions. The highest "low frequency" deposition rates for P-SiN reported by other authors are also about  $500 \text{ Å min}^{-1}$  ( $\sim 8 \text{ Å sec}^{-1}$ ), which confirms that the deposition rate ratio ( $R_{\text{MW}}/R_{\text{RF}}$ ) for P-SiN,

under comparable fabrication conditions, appears to be about 10, somewhat higher than the factor of 5 reported in section 3.2 for plasma polymers. From Fig. 5(b), we note that films of "acceptable" density ( $\rho > 2.5 \text{ g cm}^{-3}$ ), a property which appears to govern many of the other characteristics of importance to this microelectronic engineering material(21), can readily be achieved in 2.45 GHz plasma for  $T_s > 200^\circ\text{C}$ .

Finally, turning to a-Si:H, we have recently prepared many samples in the apparatus of Fig. 2. The objective was to fabricate thick films with large photoconductivities, for application in electrophotography. Samples were characterized by measuring electrical conductivity in a planar gap configuration, in the dark ( $\sigma_d$ ) and under simulated AM1 illumination ( $\sigma_{AM1}$ ). Table 1 shows a typical selection of results which are relevant to the present discussions: samples a and c were prepared in the "RF" mode [Fig. 2(b)], while b and d were prepared in the "MW" mode [Fig. 2(a)]. Pressure and ( $\text{SiH}_4/\text{Ar}$ ) flow rates were kept constant throughout at 250 mTorr and (8/42) (in sccm), respectively, while other fabrication variables were selected as shown. Two important results emerge from comparisons between sample pairs (a,b) and (c,d), namely: ( $R_{MW}/R_{RF}$ ) is about 20 in both cases, and ( $\sigma_{AM1}/\sigma_d$ ) is between one and two orders of magnitude higher for the "RF" sample materials than for their "MW" counterparts. The former observation once again confirms the above - illustrated enhancement by about an order of magnitude which results from plasma deposition in the "microwave" regime ( $v/\omega \ll 1$ ). Further, it agrees with similar observations by other workers: Curtins et al.(26) recently reported a study of a-Si:H deposition in a capacitively coupled discharge in pure  $\text{SiH}_4$ , in the frequency range  $25 < f < 150 \text{ MHz}$ . They found a sharp rise in R with increasing f, a maximum value  $R_{\text{max}} = 22 \text{ } \Omega \text{ s}^{-1}$  at  $f_{\text{max}} = 70 \text{ MHz}$ , followed by a gradual decrease in R. It is interesting to note that their  $f_{\text{max}}$  falls squarely within the transition region of Fig. 3; their subsequent drop in R, however, disagrees with our observations, and we speculate that it may be an artifact, possibly related to difficulties in impedance matching at those very high frequencies. Hudgens and Johncock (27) found even higher R values at  $f = 2450 \text{ MHz}$  than the ones we report in Table 1, namely  $> 100 \text{ } \Omega \text{ s}^{-1}$ , but their feed gas was a ( $\text{SiH}_4/\text{SiF}_4$ ) mixture.

TABLE 1. Comparison of a-Si:H samples prepared under configurations shown in Figs. 2(a) and (b)

Sample	f(MHz)	P(W)	$T_s(^{\circ}\text{C})$	$R(\text{ } \Omega \text{ s}^{-1})$	$\frac{\sigma_{AM1}}{\sigma_d}$
a	13.56	120	300	1.25	$3.7 \times 10^4$
b	2450	120	330	25	$10^3$
c	13.56	20	280	0.4	$9.5 \times 10^4$
d	2450	30	270	7	$0.8 \times 10^3$

Regarding the higher ( $\sigma_{AM1}/\sigma_d$ ) ratios obtained for RF produced a-Si:H (see Table 1), we feel this is related to ion bombardment resulting from the plasma sheath(28), which is substantially enhanced in the electroded configuration of Fig. 2(b).



#### 4. CONCLUSIONS

Theory predicts(7) that the EEDF of a high frequency sustained, low pressure plasma is modified when the parameter  $\nu/\omega$  is greater ("RF" case) or less ("MW" case) than unity. In pure argon, at a typical process pressure of 200 mTorr, the calculated value of  $\nu/2\pi$  is about 50 MHz. Assuming that a similar collision frequency value is also obtained with molecular gases, one may therefore expect to observe significant changes in a given plasma experiment (for example, thin film growth kinetics) above and below  $f = (\omega/2\pi) \approx 50$  MHz.

We have used two low pressure plasma systems, a surface wave apparatus, and an "LMP" apparatus for thin film deposition experiments in which  $f$  was, for the surface wave apparatus, strictly the only variable; with the LMP system, besides frequency, the reactor changed from an (RF) electroded to a (MW) electrodeless configuration. In all cases studied, deposition rate  $R$  was substantially lower in the "RF" regime than in the "MW" regime: ( $R_{MW}/R_{RF}$ ) values observed were about 5, 10 and 20 for deposition of plasma polymers, P-SiN and a-Si:H, respectively. These results agree with the few published data available from the literature. The obvious implication for industrial use is that the more rapid microwave plasma processing permits a given film thickness to be attained in less time, hence greater productivity of the capital-intensive plasma equipment.

#### Acknowledgements

This work has been supported in part by the Natural Sciences and Engineering Research Council of Canada (NSERC) and by the Fonds "Formation des Chercheurs et Aide à la Recherche" (FCAR) of Québec.

#### REFERENCES

1. D.L. Flamm, J. Vac. Sci. Technol. A4, 729 (1986).
2. M.R. Wertheimer and M. Moisan, J. Vac. Sci. Technol. A3, 2643 (1985).
3. A. Ricard, D. Collobert and M. Moisan, J. Phys. B: At. Mol. Phys. 16, 1657-1665 (1983).
4. R. Pantel, A. Ricard and M. Moisan, Beitr. Plasma Physik 23, 561-580 (1983).
5. A. Ricard, J. Hubert and M. Moisan, Proc. XVII Int. C. Phenomena in Ionized Gases (Contributed papers), Budapest, pp. 741-743 (1985).
6. A. Ricard, C. Barbeau, A. Besner, J. Hubert, J. Margot-Chaker, M. Moisan and G. Sauvé, contributed paper at this conference.
7. C.M. Ferreira and J. Loureiro, J. Phys. D: Appl. Phys. 17, 1175-1188 (1984).
8. C.M. Ferreira, J. Phys. D: Appl. Phys. 16, 1673-1685 (1983).
9. M. Moisan and M. Zakrzewski in Radiative processes in discharge plasmas, pp. 381-430, Plenum, New York (1987).
10. M. Chaker, M. Moisan and Z. Zakrzewski, Plasma Chem. Plasma Process. 6, 79-96 (1986).
11. M. Moisan, Z. Zakrzewski and R. Pantel, J. Phys. D: Appl. Phys. 12, 219-237 (1979).
12. M. Moisan, Z. Zakrzewski, R. Pantel and P. Leprince, IEEE Trans. Plasma Science PS-12 203-214 (1984).

13. M. Moisan, M. Chaker, Z. Zakrzewski and J. Paraszczak, J. Phys. E: Sci. Instrum. to appear (1987).
14. M. Moisan and Z. Zakrzewski, US Patent application (serial 903, 519) (1986).
15. M.R. Wertheimer, J.E. Klemberg-Sapieha and H.P. Schreiber, Thin Solid Films 115, 109 (1984).
16. R.G. Bosisio, M.R. Wertheimer, and C.F. Weissfloch. J. Phys. E 6, 628 (1973).
17. R. Claude, M. Moisan, M.R. Wertheimer and Z. Zakrzewski, Appl. Phys. Lett. 50, xxx (1987).
18. R. Claude, M. Moisan, M.R. Wertheimer, and Z. Zakrzewski, Plasma Chem. and Plasma Processing (submitted).
19. R. Groleau, J.F. Currie, M.R. Wertheimer, J.E. Klemberg-Sapieha, and Wang Ke-Ming, Thin Solid Films 136, 85-92 (1986).
20. T.S. Ramu, M.R. Wertheimer, and J.E. Klemberg-Sapieha, IEEE Trans. Electr. Insul. EI-21, 549-563, (1986).
21. Y. Tessier, J.E. Klemberg-Sapieha, S. Poulin-Dandurand, M.R. Wertheimer and S. Gujrathi, Can. J. Phys. 65, xxx (1987).
22. H. Yasuda, "Plasma Polymerization", Academic Press, New York, N.Y., 1985.
23. M. Gazicki and H. Yasuda, J. Appl. Polym. Sci. Appl. Polym. Symp. 38, 35 (1984).
24. G. Kaganowicz and J.W. Robinson, RCA Laboratories, Princeton, N.J., Tech. Rept. PRRL-84-TR-102, 8 pp; presented at 34th Can. Chem. Eng. Congress, Quebec, October 1984 (unpublished).
25. A.K. Sinha, H.J. Levinstein, T.E. Smith, G. Quintana and S.E. Haszko, J. Electrochem. Soc. 125, 601 (1978).
26. H. Curtins, N. Wyrśch and A.V. Shah, Electronics Lett. 23, 228 (1987).
27. S.J. Huggens and A.G. Johncock, Mat. Res. Soc. Symp. Proc. 49, 403 (1985).
28. B. Drevillon, J. Perrin, J.M. Sieffert, J. Huc, A. Lloret, G. de Rosny, and J.P.M. Schmidt, Appl. Phys. Lett. 42, 801 (1983).